https://doi.org/10.5194/egusphere-2026-666
Preprint. Discussion started: 5 February 2026

Design and trial implementation of a continental-scale, kilometre-resolution hourly precipitation analysis for Australia using satellite, radar and gauges

Yuhang Zhang[1], Quan J. Wang[1, 4], Andrew J. Frost[2], Jayaram Pudashine[3], Blair Trewin[3], Carlos Velasco-Forero[3], Chun-Hsu Su[3], Vincent Villani[3]

[1]Department of Infrastructure Engineering, The University of Melbourne, Parkville, VIC 3010, Australia
[2]Bureau of Meteorology, Sydney, NSW 1300, Australia
[3]Bureau of Meteorology, Melbourne, VIC 3001, Australia
[4]College of Hydrology and Water Resources, Hohai University, Nanjing 210098, China

Correspondence to: Quan J. Wang (quan.wang@unimelb.edu.au) and Andrew J. Frost (andrew.frost@bom.gov.au)

Abstract. High-resolution precipitation information is essential for hydrometeorological applications such as extreme weather monitoring, flood forecasting, and disaster risk management. Despite substantial advances in satellite, radar, and gauge observations, producing kilometre-resolution sub-daily precipitation analyses over continental domains remains challenging due to heterogeneous data availability, scale mismatches, and computational constraints. This study presents the design and trial implementation of BRAIN (blended rainfall), a continental-scale, kilometre-resolution hourly precipitation analysis for Australia. In this initial implementation, BRAIN integrates three key data sources from the Australian Bureau of Meteorology: geostationary satellite rainfall estimates from Himawari (2 km, 10 min), radar rainfall estimates (1 km, 5 min), and sub-daily rain gauge observations. The trialled system incorporates quality control, spatiotemporal aggregation, bias correction, and a simplified statistical interpolation configuration designed to balance performance with scalability at continental scale. Source contributions are weighted according to their spatial and temporal error characteristics, allowing each data type to influence the analysis where it is most informative. The trial implementation produces hourly rainfall fields at 2-km resolution across the Australian continent. Evaluation for the trial period 2022–2023 indicates that the blended analysis improves upon satellite-only, radar-only, and satellite–gauge products, outperforms the gauge-based interpolation approach currently used in flood operations, and provides more spatially coherent and detailed rainfall structures than the current daily operational product. These results demonstrate the feasibility and utility of the proposed design and trial implementation in the Australian context, with potential extension to long-term historical reconstruction and near–real-time applications. The system design is flexible and scalable, enabling future upgrades such as finer spatial and temporal resolutions and the incorporation of additional data sources. Beyond the Australian context, this study provides an additional reference for large-scale multi-source precipitation analysis at kilometre and hourly resolutions.

https://doi.org/10.5194/egusphere-2026-666
Preprint. Discussion started: 5 February 2026

1 Introduction

Precipitation is a critical component of the water cycle, exerting strong control over hydrological processes and acting as a primary driver of flooding, which poses significant risks to infrastructure and human safety (Prein et al., 2017). However, accurately characterising precipitation fields, particularly at high spatial and temporal resolutions, remains challenging due to their pronounced variability across scales (Nishant et al., 2022; Zhang et al., 2021a). For example, rain gauges, while reliable for point-based measurements, struggle to capture spatial variability, especially in regions with sparse observation networks (Villarini et al., 2008). Weather radars provide high-resolution data with broader spatial coverage but are typically concentrated in densely populated areas, leaving large remote regions unmonitored (e.g., Zhang et al., 2025). Satellites-based precipitation products provide near-global coverage and high temporal sampling, but their estimates are subject to retrieval uncertainties arising from indirect measurement principles and algorithmic assumptions (e.g., Sun et al., 2018; Zhang et al., 2021b, c). Reanalysis products, which combine numerical weather prediction models with diverse observations, provide spatially and temporally complete precipitation fields, but their resolution and accuracy depend on model configuration and data assimilation assumptions (e.g., Su et al., 2019, 2021, 2025). Integrating information from multiple sources through blending offers a pathway to leverage the complementary strengths of each data source, mitigate their individual limitations, and better represent precipitation variability across space and time (e.g., Beck et al., 2017, 2019).

A range of approaches have been developed for multi-source precipitation blending (e.g., Xu et al., 2024; Zhang et al., 2025). For example, performance-based averaging methods derive weights for non-gauge data sources from gauge-based skill metrics and apply them in a grid-aligned manner, but their applicability may be limited in regions with very sparse gauge coverage. Triple collocation-based approach provides a gauge-independent alternative by estimating weights from independent data sources (e.g., Dong et al., 2022; Koster et al., 2021; Xu et al., 2020); however, both approaches typically require spatially complete datasets and assign fixed source weights over time, limiting their applicability under heterogeneous data coverage, such as mixtures of spatially incomplete gridded fields and point observations. Multifractal blending methods aim to combine precipitation information across spatial scales (e.g., Imhoff et al., 2023; Renzullo et al., 2017), but their implementation can be challenging when consistent scaling behaviour is not evident in the input data. More recently, machine learning–based approaches have been explored (e.g., Gavahi et al., 2023; Kossieris et al., 2024; Xu et al., 2024), in which non-gauge data sources are treated as input features and model relationships are learned using gauge observations as targets; while offering high flexibility, these approaches often have limited interpretability and substantial computational demands, which have constrained their adoption in operational precipitation analysis. In addition, all above approaches typically do not assimilate gauge observations directly as a primary data source in the blending step, which can limit performance in gauge-rich regions where point observations provide the most accurate precipitation information.

Compared with the approaches discussed above, statistical interpolation, also known as optimal interpolation, is a statistical method with several properties that are well suited to multi-source precipitation blending (e.g., Bhargava and Danard, 1994; Chua et al., 2022a, 2023; Fortin et al., 2018; Gandin, 1963; Mahfouf et al., 2007; Shen et al., 2014a, 2018). A defining

https://doi.org/10.5194/egusphere-2026-666
Preprint. Discussion started: 5 February 2026

feature of statistical interpolation is that rain gauge observations are explicitly assimilated as a primary data source, rather than being used only indirectly for weight estimation, bias correction, or model training. The grid-wise, time-step-wise formulation combines a spatially complete background field with observational increments weighted according to error characteristics and spatial proximity. This structure enables the flexible integration of point and gridded observations while accommodating spatial and temporal data gaps, making statistical interpolation well suited for large-scale precipitation analysis in conditions with heterogeneous data availability. Building on these properties, multi-source precipitation analysis or reanalysis systems have been developed and implemented in several countries in the world, including the United States (e.g., Xie et al., 2010), Canada (e.g., Fortin et al., 2015, 2018; Khedhaouiria et al., 2020, 2022; Mahfouf et al., 2007), the United Kingdom (e.g., Yu et al., 2020), China (e.g., Shen et al., 2014a, 2018; Xie and Xiong, 2011), and France (e.g., Hyfte et al., 2023), with a wide range of spatial and temporal resolutions. In practice, the achievable spatial and temporal resolution of such systems is largely constrained by the data source used for background field. For example, systems based on global satellite products and NWP outputs commonly at spatial resolutions of around 10 km unless additional interpolation or downscaling is applied, with temporal resolutions typically ranging from hourly to several-hourly intervals, depending on data availability and computational cost. Although these systems generally follow similar blending principles, each implementation must be tailored to regional data availability, blending configuration, computational capacity, and operational requirements, and must be maintained through routine updates as observing systems evolve.

In Australia, several gridded precipitation products based on daily gauge observations have been developed to support climate and water-related applications (e.g., Jeffrey et al. 2001; Jones et al. 2009; Evans et al. 2020). For example, the Australian Gridded Climate Data (AGCD) product, formerly known as the Australian Water Availability Project (AWAP) product (Jones et al., 2009) provides an operational 5-km daily rainfall dataset that is widely used and is being progressively upgraded towards higher resolution (i.e., 1 km). Despite these advances, there is currently no national operational gridded rainfall product that provides high-resolution precipitation at sub-daily timescales (e.g., hourly). For flood modelling and forecasting, sub-daily gauge observations therefore remain the primary data source, with inverse distance weighting (IDW) interpolation currently used operationally to estimate catchment-scale rainfall. While radar-based rainfall products (Seed et al., 2007) offer high spatial and temporal resolution, their limited coverage leaves a substantial fraction of the Australian land area unmonitored (approximately 28% as of year 2023), particularly in remote regions (see Fig. 1c). Satellite-derived sub-daily precipitation estimates are also available, but their relatively coarse resolution (e.g., 10 km) and uncertainty constrain their suitability compared with gauge-based analyses (Islam et al., 2020).

The lack of a national, high-resolution sub-daily rainfall product highlights the need for a multi-source precipitation analysis for Australia (Nishant et al., 2022). Several experimental efforts have sought to address this gap. Disaggregation approaches infer sub-daily rainfall from daily products using high-frequency data such as reanalysis (Acharya et al., 2022), but their accuracy depends on the ability of reanalysis to realistically represent sub-daily precipitation and is further limited by data latency for near–real-time applications (Su et al., 2024). Blending-based studies have demonstrated the potential of

https://doi.org/10.5194/egusphere-2026-666
Preprint. Discussion started: 5 February 2026

integrating multiple data sources, including satellite–gauge merging using statistical interpolation at the monthly scale Chua et al. (2022a, b) and catchment-scale blending of NWP, satellite, and radar data using multifractal methods (Renzullo et al., 2017). However, these efforts have not been extended to a national-scale, kilometre-resolution, sub-daily rainfall product.

Recently, the Australian Bureau of Meteorology (hereafter, the Bureau) has implemented the Himawari-based Convective Rainfall Rate from Cloud Physical Properties (CRRPH) product, which offers markedly higher spatial (2 km) and temporal (10 min) resolution than existing global satellite products such as the Integrated Multi-satellite Retrievals for Global Precipitation Measurement (IMERG, 10 km and 30 min), with frequent updates (15 min) suitable for near–real-time applications (Bureau of Meteorology, 2024). This provides a promising foundation for constructing kilometre-resolution, sub-daily precipitation fields at the national scale.

As part of recent national efforts to advance high-resolution precipitation analysis, the Bureau has initiated the *Next Generation Rainfall Project*. The project aims to develop a new generation of rainfall products to support both historical applications, such as climate analysis and hydrological model calibration, and near–real-time operational uses, including flood forecasting and disaster response. Within this context, this paper presents the design and trial national implementation of BRAIN (Blended Rainfall). BRAIN is a multi-source precipitation analysis that produces hourly rainfall fields at 2-km resolution across Australia by integrating satellite, radar, and sub-daily gauge observations within a statistical interpolation framework.

The study makes several key contributions:

(i) It systematically examines the role of the latest Himawari CRRPH satellite rainfall product as a high-resolution background field and investigates its interaction with radar and sub-daily gauge observations within the blended analysis, building on recent advances by the Bureau in satellite-based rainfall estimation.

(ii) It presents the first continental-scale trial implementation in Australia that integrates all currently available and operationally manageable satellite, radar, and gauge observations within a unified framework, extending previous multi-source efforts toward an operationally viable national product.

(iii) It applies and tailors statistical interpolation theory to Australian observational and computational constraints, including the adoption of an error-informed localisation strategy and a simplified nearest-point representation for radar observations, thereby enabling scalable, grid-cell-wise and time-step-wise blending at kilometre and hourly resolutions with minimal computational overhead.

(iv) It evaluates blending performance from multiple complementary perspectives, including comparisons against single-source fields, two-source blending configurations, and existing operational products and approaches, demonstrating the feasibility of producing consistent kilometre-resolution, hourly rainfall analyses at national scale.

The BRAIN framework is designed to be extensible, scalable, and transferable. It allows the future incorporation of additional data sources, including alternative satellite products, numerical weather prediction (NWP) or reanalysis outputs,

https://doi.org/10.5194/egusphere-2026-666
Preprint. Discussion started: 5 February 2026

and daily gauge observations. The framework also supports adaptation to finer spatial or temporal resolutions (e.g., 1 km and 30 min) as operational and research needs evolve and as computational resources increase. Beyond the Australian context, BRAIN provides a practical reference for large-scale multi-source precipitation analysis at kilometre and hourly resolutions. It complements existing regional-, national-, and basin-scale implementations and contributes to a broader understanding of multi-source precipitation performance under heterogeneous observational conditions.

2 Data sources

Many different data sources are possible for use in generating a blended precipitation product for Australia. In the first instance, we use three Bureau-managed precipitation observation data sources for blending:

- In situ gauges (15/30-min data aggregated to hourly) from the Bureau and those supplied operationally through other jurisdictional agencies to support the Bureau's flood forecasting and warning responsibilities.
- Radar rainfall rates (5-min, 1-km grid) from the Bureau's nationally owned network.
- Satellite estimates processed from Himawari (10-min, 2-km grid).

As detailed further below, these data feeds were chosen to build the service because: (1) All three data sources (in situ gauges, radar, and satellite) are currently operational, ensuring both feasibility and immediate applicability; (2) Among these, in situ gauge data are already used operationally to support national flood forecasting services and serve as the primary reference for validation. Additional datasets are being considered for future upgrades (see Section 5 for further directions). The 2022–2023 period was used for trial development to provide an indication of near-current performance.

https://doi.org/10.5194/egusphere-2026-666
Preprint. Discussion started: 5 February 2026

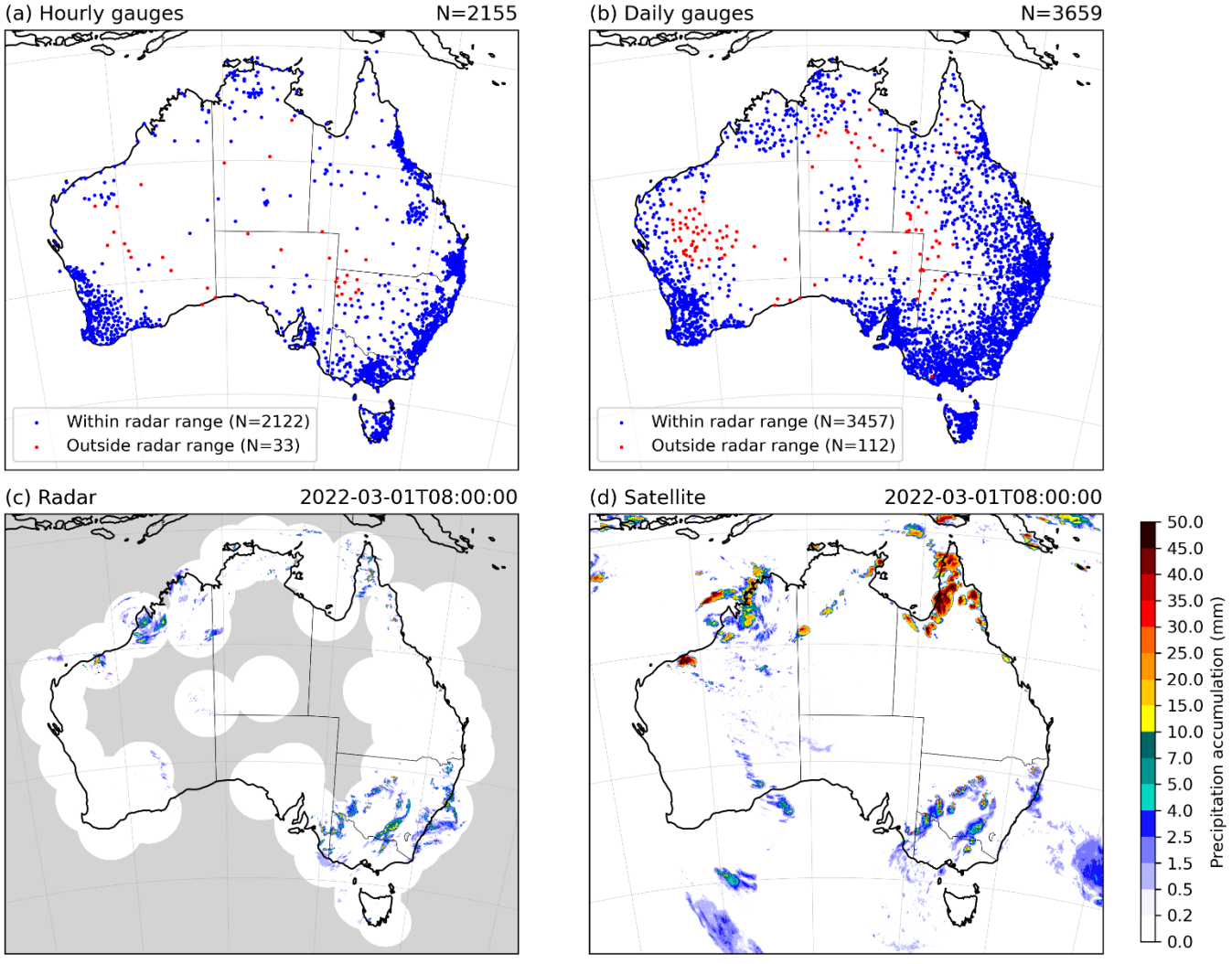

Figure 1. Spatial distribution and coverage of the data sources used in this study: (a) hourly gauges (aggregated from sub-daily) (N=2,155) categorized into those within maximum radar range (N=2,122, blue) and outside maximum radar range (N=33, red), (b) daily gauges (N=3,659) similarly categorized within maximum radar range (N=3,457, blue) and outside maximum radar range (N=112, red), (c) radar-based precipitation product showing the calibrated hourly rainfall accumulation at the continental scale for 0800 UTC on 1 March 2022. The radar has a maximum range of approximately 300 km with a 1-km spatial resolution, and (d) satellite-based precipitation product (CRRPH) showing the hourly rainfall accumulation at the same time and spatial domain. The satellite product provides seamless spatial coverage with a 2-km spatial resolution.

https://doi.org/10.5194/egusphere-2026-666
Preprint. Discussion started: 5 February 2026

2.1 In situ observations

A total of 2,155 sub-daily (aggregated to hourly) (Fig. 1a) and 3,659 independent daily (Fig. 1b) rain gauge stations (Bureau of Meteorology, 2025) were used in this study. The hourly gauges, sourced from both automatic weather stations and flood warning stations, were recorded at sub-hourly intervals and served as the primary input for the blending process. The daily gauges, obtained primarily from human-recorded observations, provided an independent evaluation dataset for the final blended product. To prevent redundancy, any gauge present in both datasets was retained only in the hourly dataset. Both the hourly and daily datasets were subjected to rigorous quality control procedures, including checks for extreme high values comparing with gridded design rainfall fields; spatial intercomparisons to detect anomalous high values, or prolonged periods of zero values which may indicate an instrument failure or gauge blockage; intercomparisons between sub-daily and daily data in cases where these are separately stored; and large numbers of successive identical non-zero values. The network density varies significantly for hourly gauges (Fig. 1a), with some areas—particularly along the populated and flood-prone Great Dividing Range in eastern Australia—having dense coverage, while others have little to no data. In contrast, daily gauges (Fig. 1b) are more evenly distributed, though substantial data voids remain, particularly in the arid and sparsely populated western interior.

An additional independent hourly dataset (approximately 2000 stations) was collated after completion of the main analyses and used for supplementary evaluation. The spatial distribution of these hourly gauge stations is shown in Figure S13.

2.2 Radar-based observations

Radar rainfall estimates (Bureau of Meteorology, 2022) were obtained from the Bureau's operational Rainfields system, which provides real-time data at a 1-km/5-min resolution. The system offers both raw and calibrated radar rainfall rates. Raw rainfall rates are derived using reflectivity–rainfall rate (Z–R) relationships, which are established for each radar based on long-term historical data. Calibrated rainfall rates are then generated by applying dynamic bias correction to the raw estimates using nearby gauge observations within a 150-km radius over a 15-min time window, employing a Kalman filtering approach (Chumchean et al., 2006). By incorporating real-time gauge data, calibrated radar rainfall rates provide an additional refinement to the Z-R-based estimates, ensuring adjustments to current conditions that may deviate from the historical period used to derive the Z-R relationships.

In this study, we used hourly radar accumulations derived from 5-min calibrated radar rain rates as a blending input for the target hourly resolution. However, we recalibrated the radar data using gauges within a 300-km radius over a 1-hour window to better match the hourly target timescale, improving accuracy by incorporating more gauges. We refer to the operational calibrated product as R0 and the recalibrated version as R1. In addition, to match the spatial resolution with satellite data, the original 1-km radar grids were aggregated to 2 km. Figure 1c shows an example of the calibrated radar rainfall hourly accumulation (R1) at a continental scale, recorded at 0800 UTC on 1 March 2022.

https://doi.org/10.5194/egusphere-2026-666
Preprint. Discussion started: 5 February 2026

2.3 Satellite-based observations

The Himawari-based CRRPH v2.1 product (Bureau of Meteorology, 2024) was selected as background filed for this study because it provides continental coverage at 2-km spatial and 10-min temporal resolution, helping to compensate for gaps in the ground-based network. The product is derived from the Japanese Himawari-8/9 geostationary satellites, which carry the Advanced Himawari Imager (AHI) and provide multi-spectral observations of cloud and atmospheric properties over the Australian region. CRRPH exploits the high-frequency, multi-channel infrared observations from AHI to infer convective rainfall rates based on cloud physical properties, including cloud optical depth and effective radius, which are indicative of convective intensity.

The CRRPH product is available from 2015 onwards and is updated operationally with a latency of approximately 15 minutes, making it suitable for near–real-time applications. In this study, the native 2-km spatial resolution of CRRPH was adopted as the target grid for blending, thereby defining a common spatial standard across all input datasets. This choice avoids additional spatial resampling of the satellite field and reduces potential interpolation-induced errors. Temporally, the 10-min CRRPH rainfall rates were aggregated to hourly accumulations prior to blending to ensure consistency with other data sources and downstream hydrological applications.

Figure 1d illustrates an example of the CRRPH hourly rainfall accumulation at the continental scale at 0800 UTC on 1 March 2022, highlighting its ability to represent large-scale precipitation patterns with fine spatial detail. As with other satellite-based precipitation products, CRRPH rainfall estimates are subject to systematic biases. To mitigate these effects, a mean bias correction was applied using a gauge-based adjustment approach (Chumchean et al., 2006), consistent with the procedure adopted for radar rainfall estimates. Further details of the bias correction methodology are provided in Section 3.3.

3 Methods

3.1 Workflow

The multi-source blending workflow (Fig. 2) integrates satellite, radar, and gauge data through a multi-step process to produce a high-resolution blended rainfall product. After temporal/spatial aggregation, quality control, and bias correction, satellite data serve as the background, radar data as the first-layer observations, and gauge data as the second-layer observations. These inputs are then combined using the multi-source statistical interpolation framework to generate the final blended rainfall (BRAIN) product. Some key steps are detailed in the following subsections.

https://doi.org/10.5194/egusphere-2026-666
Preprint. Discussion started: 5 February 2026

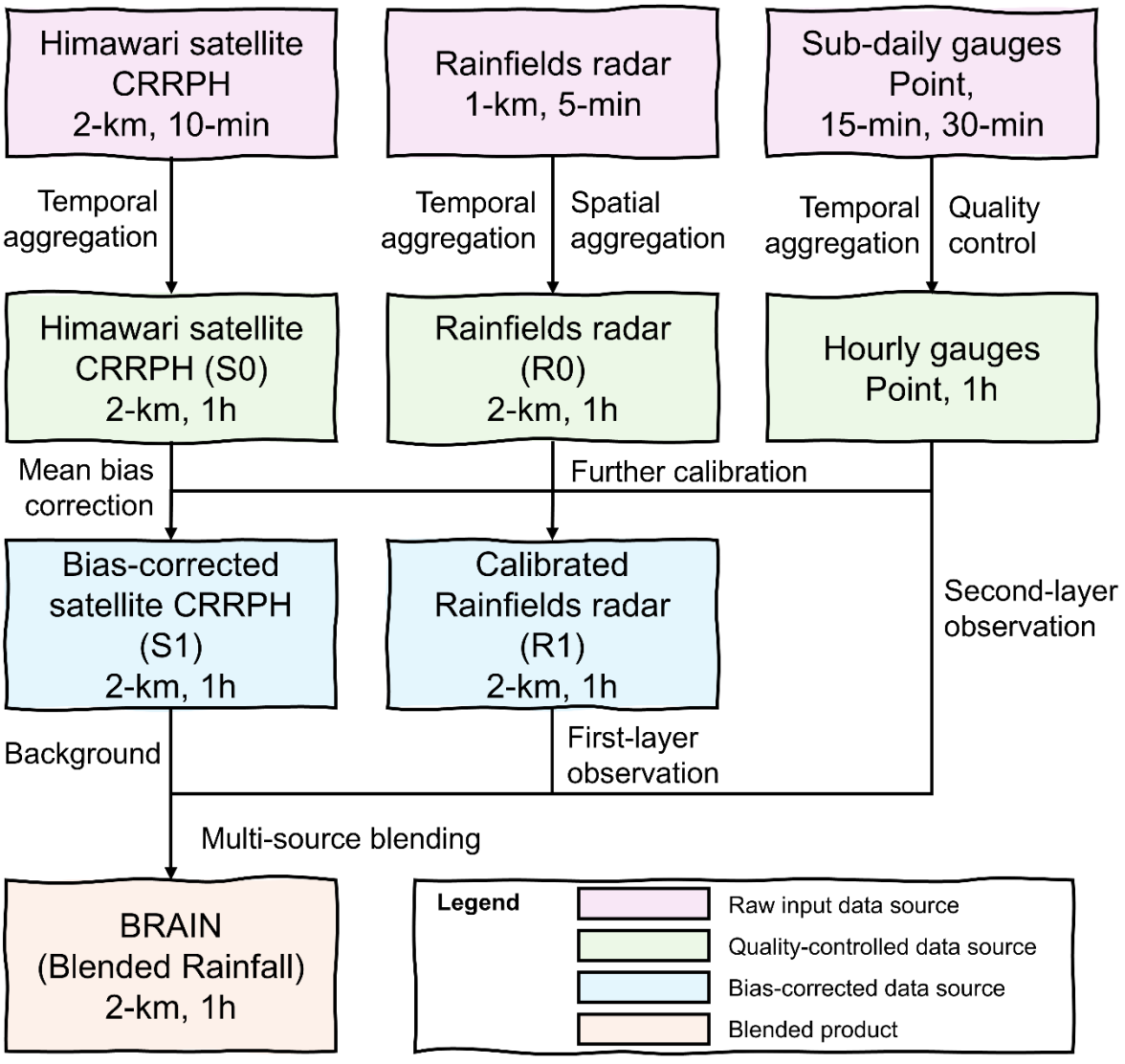

Figure 2. Workflow of the multi-source statistical interpolation blending process used in BRAIN (Blended Rainfall) analysis. The inputs include Himawari satellite CRRPH data (2-km, 10-min), Rainfields radar data (1-km, 5-min), and sub-daily gauge observations (point data, 15/30-min). The workflow includes temporal aggregation for satellite, radar and gauge data, spatial aggregation for radar data, and quality control for gauge data. After bias correction, the satellite data serves as background, the radar data serve as the first-layer observations, and the gauge data act as second-layer observations. The trialled implementation of the system integrates these inputs to generate the final blended rainfall product (BRAIN) with a 2-km spatial and 1-hour temporal resolution.

https://doi.org/10.5194/egusphere-2026-666
Preprint. Discussion started: 5 February 2026

3.2 Multi-source statistical interpolation

A range of approaches can be selected for producing blended gridded datasets (e.g., Yin et al. 2021; Gavahi et al. 2023; Khedhaouiria et al. 2022; Chappell et al. 2013; Shen et al. 2014; Yu et al. 2020). Statistical interpolation is a widely used interpolation method in many meteorological organisations (e.g., Mitchell et al. 1990; Huang et al. 1997; De Mey 1994; Lorenc et al. 1991) for blending or assimilating observations with weather models, particularly before the development of more advanced variational methods (e.g., Gauthier et al. 2007; Rawlins et al. 2007; Rabier et al. 2000; Rabier 2005). More recently, it has been widely applied to precipitation interpolation and blending (e.g., Xie and Xiong 2011; Yu et al. 2020; Chua et al. 2022a; Mahfouf et al. 2007).

Statistical interpolation enables the integration of multi-source precipitation data by updating a *background* estimate—in this case, the satellite-derived first guess—based on *observations* (gauge/radar fields) to generate an *analysis*, with adjustments weighted according to the estimated error characteristics of each data source. The method assumes Gaussian error distributions, which may not strictly hold for precipitation but are commonly used approximations to avoid added complexity from data transformation, while bias correction is applied to both satellite and radar data to help satisfy the assumption of unbiased errors. Statistical interpolation operates as an iterative, grid-based analysis adjusting each target grid cell using observations within a predefined search radius (e.g., 200 km).

For a given target grid cell k, the analysis value is computed as:

$$A_k = B_k + \sum_{i=1}^{n} w_i \cdot (O_i - B_i) \quad (1)$$

where A_k is the analysis value, B_k is the background value, O_i is the observational value at a nearby location i, and B_i is the corresponding background value, n is the total number of nearby observations. The term $O_i - B_i$ represents the observational increment, and w_i are the weights assigned to each observation.

The analysis error is then determined as the difference between the "true value" and the analysis value:

$$E_k^2 = (T_k - A_k)^2 = [T_k - B_k - \sum_{i=1}^{n} w_i \cdot (O_i - B_i)]^2 \quad (2)$$

By defining the background error $f_i = T_i - B_i$ and observational error $\varepsilon_i = O_i - T_i$, the analysis error equation can be rewritten as:

$$E_k^2 = [f_k - \sum_{i=0}^{n} w_i \cdot (f_i + \varepsilon_i)]^2 \quad (3)$$

Minimizing this error allows us to optimally assign weights to nearby observations, yielding the most statistically accurate estimate for each target grid cell. To solve this optimization problem, we take the partial derivative of E_k^2 with respect to each w_i and set it to zero, which leads to the following equation:

$$\sum_{j=1}^{n} (f_i + \varepsilon_i)\,(f_j + \varepsilon_j) w_i = f_k (f_i + \varepsilon_i),\ i = 1,2,\dots,n \quad (4)$$

https://doi.org/10.5194/egusphere-2026-666
Preprint. Discussion started: 5 February 2026

By expanding and expressing the above equation in normalised form:

$$\sum_{j=1}^{n}\left(\mu_{ij}+\tau_{ij}\sigma_j+\tau_{ji}\sigma_i+\rho_{ij}\sigma_i\sigma_j\right)w_i'=\mu_{ki}+\tau_{ki}\sigma_i,\ i=1,2,\dots,n \quad (5)$$

where:

- $\mu_{ij}=f_if_j/\left(f_i^{\,2}f_j^{\,2}\right)^{\frac{1}{2}}, \mu_{ij}\in\mathbb{R}^{n\times n}$ is the background (satellite) error correlation between the *i*th and *j*th observational locations. Similarly, $\mu_{ki}\in\mathbb{R}^{1\times n}$ is the background error correlation between the target grid cell *k* and the *i*th observational location.
- $\tau_{ij}=f_i\varepsilon_j/\left(f_i^{\,2}\varepsilon_j^{\,2}\right)^{\frac{1}{2}}, \tau_{ij}\in\mathbb{R}^{n\times n}$ is the correlation between the background error at the *i*th location and the observational error at *j*th location. Similarly, τ_{ki} is the correlation between the background error at the target grid cell *k* and the observational error at the *i*th observational location.
- $\rho_{ij}=\varepsilon_i\varepsilon_j/\left(\varepsilon_i^{\,2}\varepsilon_j^{\,2}\right)^{\frac{1}{2}}, \rho_{ij}\in\mathbb{R}^{n\times n}$ is the observational error correlation between the *i*th and *j*th observational locations.
- $\sigma_i=\left(\varepsilon_i^{\,2}/f_i^{\,2}\right)^{\frac{1}{2}}, \sigma_i\in\mathbb{R}^{n\times 1}$ is the ratio of the standard deviation of observational error to the standard deviation of background error at the *i*th observational location.
- $w_i'=w_i\left(f_i^{\,2}/f_k^{\,2}\right)^{\frac{1}{2}}, w_i'\in\mathbb{R}^{n\times 1}$ is adjusted weight accounting for differences in background error across between the *i*th observational location and target grid cell *k*.

This system of linear equations is solved to determine the optimal weights w_i, which are used to obtain the best precipitation estimate at each target grid cell by optimally combining satellite, radar, and gauge data. These equations require knowledge of the background error correlation (μ_{ij}, μ_{ki}), background-to-observation error correlations (τ_{ij}, τ_{ki}), observational error correlations (ρ_{ij}), the ratio of observational to background error variances (σ_i), and the spatial variation of background errors ($f_i^{\,2}/f_k^{\,2}$).

The background error correlation is typically derived from an analytical function (e.g., Bergman 1978; Xie and Xiong 2011; Yu et al. 2020), while background-to-observation error correlations are assumed to be zero, as different sensor systems are considered independent. Similarly, the observational-to-background error variance ratio is estimated separately for satellite, radar, and gauge data using analytical functions (e.g., Bergman 1978; Xie and Xiong 2011; Yu et al. 2020), with the corresponding ratios computed between different data sources. The most challenging part of statistical interpolation is determining the observational error correlations (ρ_{ij}), as it requires accounting for the number of observations in different cases and their respective sensor systems, particularly as the number of data sources increase.

In this study, both gauge and radar are incorporated as observations. Since radar and gauge data originate from different sensor systems, they are simply treated as independent. Furthermore, gauges at different locations are also assumed to be

https://doi.org/10.5194/egusphere-2026-666
Preprint. Discussion started: 5 February 2026

independent. Accordingly, radar–gauge and gauge–gauge observational error correlations are set to zero. However, incorporating radar-to-radar error correlations into the linear equations (i.e., Eq. (5)) is impractical, as a single target grid cell may involve hundreds of radar points within the influence radius (e.g., 200 km), leading to high computational cost and potential matrix rank deficiency.

To address this issue, an error-informed localisation strategy is adopted within the statistical interpolation framework. Specifically, a highly efficient implementation is introduced in which only the nearest radar grid cell to each target grid cell is retained as a supplementary observation. This nearest-point approximation reflects a deliberate selection strategy that prioritises the most locally relevant radar information while avoiding dilution by redundant contributions. As a result, this approach enables scalable, grid-cell-wise blending suitable for continental-scale precipitation analysis at kilometre spatial resolution and hourly temporal resolution under practical computational constraints.

The design offers several advantages. First, it substantially reduces computational complexity by avoiding redundancy in the statistical interpolation linear system, which is particularly important for continental-scale applications in Australia involving more than five million grid cells. Second, it removes the need to explicitly model radar-to-radar error correlations, thereby simplifying the modelling chain and reducing the number of processing steps. Third, by constraining the spatial influence of radar observations, the approach limits error extrapolation, an important consideration given the directional and range-dependent nature of radar errors. Finally, despite its simplicity, the strategy allows radar observations to contribute effectively both within and outside radar coverage, ensuring consistency and spatial continuity across data sources in the blended rainfall fields.

Following the above strategy and design, we solve the simplified system of linear equations from Eq. (5):

$$\sum_{j=1}^{n}\left(\mu_{ij}+\rho_{ij}\sigma_i\sigma_j\right)w_i'=\mu_{ki},\ i=1,2,\dots,n \tag{6}$$

where n represents the number of available observations within the influence radius (set to 200 km in this study) for a specific target grid cell. The number of observations varies by case. These include: (1) a single radar grid cell, (2) a single gauge, (3) multiple gauges, (4) one or more gauges combined with one radar grid cell, and (5) no available gauge or radar observations. For the multi-gauge case, a maximum of 20 gauges is used. These correspond to the closest gauges within the 200 km radius. When a radar observation is also present, the total number of observations does not exceed 21. This system size remains computationally manageable.

In Eq. (5), the background-to-observation error correlation terms including τ_{ij}, τ_{ji} and τ_{ki}, are assumed to be zero. This assumption reflects the negligible correlation between background and observation errors and leads directly to the simplified formulation in Eq. (6). And then gauge-to-gauge error correlations are assumed to be zero between different locations and equal to one at the same location. Under the nearest-point approximation, only a single radar observation is included. Gauge–radar error correlations are also assumed to be negligible. Under these assumptions, the error correlation matrix ρ_{ij}

https://doi.org/10.5194/egusphere-2026-666
Preprint. Discussion started: 5 February 2026

reduces to the identity matrix ($\rho_{ij} = \mathbf{I}$). The radar observation contributes only through its self-correlation, which is represented by the final diagonal element and set to one.

With these simplifications, the linear system remains computationally efficient in all cases. This efficiency is essential for continental-scale applications and is particularly important for real-time monitoring and nowcasting. It also supports the efficient production and iterative refinement of long-term historical products at high spatial and temporal resolution. Once the weights are determined, the analysis value at the target grid cell is computed using Eq. (1), yielding the optimal precipitation estimate.

3.3 Mean bias correction of satellite and radar precipitation estimations

Bias correction for satellite and radar data followed a method similar to that used for operational radar calibration via a Kalman filter, as described by Chumchean et al. (2006), but adapted to the target hourly timescale. Data were first extracted at gauge locations, ensuring consistent gauge selection across satellite and radar fields, except for gauges located outside the radar range where no radar information is available. Bias at each location was estimated using a Kalman filter with an AR(1) model to capture temporal dependence, then interpolated spatially using ordinary kriging. The resulting bias field was applied multiplicatively to the raw product to produce the corrected product.

The calibrated radar estimates (R1) used in this study differ from the operational Rainfields product (R0) in both temporal and spatial configuration. R0 applies bias correction using gauges within a 150-km radius and a 15-min window, constrained by latency and the short update interval. In contrast, R1 uses gauges within a 300-km radius and a 1-hour window, allowing more gauges to be included and improving correction accuracy. This approach ensures consistent configurations for satellite and radar bias correction by using the same set of gauges (accounting for radar range) in both cases. However, this case is tailored to the Australian radar system; for different radar operation systems, adjustments can be made based on their own configuration and production objectives.

3.4 Error characterisation

Error characterisation is essential for determining observation weights. It involves estimating the error variance and correlation of each data source for both gauged and ungauged locations. Ideally, this error analysis should be conducted at each target grid cell to obtain accurate error estimates. For gauged locations, this task is relatively straightforward, as gauge observations can be used as ground truth to estimate the error characteristics of the background and observational inputs. However, for ungauged grid locations (99.9% of the 2-km land grid cells nationally), the process becomes challenging due to the absence of gauge observations. To address this, incorporating spatial and temporal windows to gather sufficient samples is a common approach. For example, for a target grid cell, one might analyse data from one month before the target hourly time step and include available hourly gauges within a 10° × 10° longitude-latitude extent. However, implementing these configurations in practice is infeasible at the km-scale used in this study, as a 2 km resolution product in Australia involves

https://doi.org/10.5194/egusphere-2026-666
Preprint. Discussion started: 5 February 2026

over 5 million grid cells (including ocean areas of interest, see Fig. 1d). Additionally, the sparse distribution of hourly gauges necessitates adaptive spatial and temporal windows rather than fixed ones, requiring adjustments based on the availability of hourly gauges for each specific grid cell and time step. This approach would demand substantial effort and fine-tuning.

To simplify the process, we estimated regional error characteristics by dividing the analysis into subregions. Satellite errors showed latitude dependence, with greater errors occurring in tropical northern Australia. In contrast, radar error characteristics are more radar-specific, with errors differing depending on local topography around the radar range, differences in the radar type and hardware configuration, and site-specific Z-R parameters. In addition, the bias correction of radar data helped reduce range-dependent error to some extent. For simplicity and consistency, in the first instance, the same regional divisions were applied to both the satellite and radar error characterisations. Specifically, the Australian domain was divided into tropical, subtropical, and temperate subregions. Curves for error variances and error correlations were fitted within each subregion. Error characteristics were calculated using data from gauged locations and then applied to ungauged locations within the same subregion.

For error variances, we calculated the squared differences between satellite (or radar) estimates and gauge observations. The error variance increases with precipitation intensity, making this relationship suitable for fitting error variance curves. To capture this, precipitation intensities were divided into bins, and within each bin, the mean squared error between satellite (or radar) estimates and gauge observations was calculated as the error variance. This analysis showed that error variance is a function of precipitation intensity. Various curve-fitting models were tested to represent the scatter, and the optimised parameters for the best-fitting curves were obtained.

For error correlations, pairs of satellite (or radar) estimates and gauge observations were collected, and the error correlation was calculated for each pair along with their corresponding distance. Distances were similarly divided into bins, and within each bin, the mean error correlation was calculated. This revealed that error correlation is a function of distance. As with error variances, different curve-fitting models were applied to the scatter, and the optimised parameters for the best-fitting curves were determined.

3.5 Evaluation strategies

As the overarching goal is to develop a blended precipitation product using three sources (i.e., satellite, radar and gauge) and transition it to operational use, we have two main objectives. First, the blended three-source product (i.e., satellite-radar-gauge) should demonstrate improvements over any individual source (i.e., satellite, radar and gauge) as well as over two-source combinations (i.e., satellite-gauge blending), confirming that the blending process effectively leverages the strengths of all datasets. In particular, the blended product should outperform the current operational method, which relies on inverse distance weighting (IDW) interpolation of sub-daily gauges, thereby indicating its potential for operational adoption. Second, the sub-daily blended product should perform comparably to, or ideally better than, the current daily operational product (i.e.,

https://doi.org/10.5194/egusphere-2026-666
Preprint. Discussion started: 5 February 2026

AGCD). These objectives ensure that the blended product is robust, accurate, and operationally viable, addressing the limitations of individual sources and existing interpolation techniques while aligning with current operational practices. To achieve these objectives, we used the following data sources for evaluation:

- Hourly gauges (Fig. 1a): Used in 20-fold cross-validation to assess hourly performance of both the blended BRAIN product and IDW interpolation.
- Daily gauges (Fig. 1b): Independent of the hourly dataset, used for an additional and complementary assessment.
- IDW-based interpolation: Included as a benchmark for comparison with the blended product, as it is currently used as the operational method in Australia for estimating hourly rainfall.
- AGCD daily gridded product: Used for comparison at the daily scale as it is the operational product in Australia (Jones et al. 2009).

Cross-validation was applied to both blended BRAIN product and IDW-based interpolation using hourly gauge data. A 20-fold approach was used, with 95% of the data for blending/interpolation and 5% for validation in each fold, repeated 20 times without replacement. For the statistical evaluation of the blended product, we primarily used correlation and root mean square error (RMSE) as performance metrics. Correlation measures the strength and direction of the linear relationship between the blended product and gauge observations. Higher correlation values indicate better agreement, with values closer to 1 representing stronger performance. RMSE quantifies the magnitude of errors between the blended product and gauge observations. Lower RMSE values indicate smaller errors and better overall accuracy of the blended product. In addition, bias was included to quantify the systematic overestimation or underestimation of the blended product relative to observations. All metrics were calculated individually for each gauge to ensure a detailed assessment of performance across all locations. The spatial match between the gridded data and gauge locations was established using nearest interpolation. For the trialled implementation, a two-year dataset from 2022 to 2023 was used in this study.

An additional independent hourly dataset from approximately 2000 gauges (see Fig. S13) was collated after completion of the main analyses and used for supplementary evaluation. This independent dataset provides additional and robust external evidence supporting the reliability of the evaluation outcomes derived from the primary hourly cross-validation analysis.

There are several existing global precipitation products (e.g., Beck et al., 2019; Ma et al., 2025) that could be used for comparison and evaluation of the blended BRAIN product. However, these products are developed for different objectives and application contexts, and therefore such comparisons are not considered in this study. First, most global products have either coarser spatial resolution or lower temporal resolution than BRAIN, which limits the meaningfulness of direct comparisons at same spatial and temporal resolutions. Second, the BRAIN product is explicitly designed as an operational product for Australia, with an update latency of less than one hour. This near-real-time capability represents a key advantage that is not shared by most global products. Third, the BRAIN framework incorporates a large number of sub-daily gauge observations available in Australia as a core data source. Many of these gauges have not been used in the development of

https://doi.org/10.5194/egusphere-2026-666
Preprint. Discussion started: 5 February 2026

existing global products, resulting in a fundamentally different observational basis. Given these differences in spatial and temporal resolution, operational objectives, and observational inputs, direct comparison with global precipitation products would be neither fully fair nor particularly informative. Instead, the focus of this study is placed on evaluating the internal consistency, added value, and performance gains of the BRAIN framework relative to its constituent data sources and blending configurations. On this basis, we expect the blended BRAIN product to demonstrate clear advantages and improved performance within its intended operational and regional context.

4 Results and discussion

4.1 Satellite and radar bias correction

Figure 3 demonstrates the spatial and statistical improvements in mean bias error for satellite and radar precipitation data after bias correction, evaluated against hourly gauge observations across Australia during the 2022–2023 period.

Before correction, satellite data (Fig. 3a) exhibits a clear latitude-dependent bias pattern, with notable overestimation in tropical areas that decreases progressively in subtropical and temperate regions (also see Fig. S1a). The corresponding histogram (Fig. 3e) reveals a highly positive-skewed distribution, indicating substantial overestimation across most hourly gauges. After correction, biases (Fig. 3b) are significantly reduced where initial errors were large, and the error distribution (Fig. 3f and Fig. S1c) becomes narrower and more symmetric.

For radar data, the operational Rainfields product (R0, Fig. 3c) shows no clear latitude-dependent bias but exhibits localised errors, particularly over the eastern coast (also see Fig. S1b). The histogram (Fig. 3g) indicates a general tendency toward overestimation. After the bias correction used in this study (R1, Fig. 3d), spatial consistency improves, and large biases are reduced. The error distribution (Fig. 3h and Fig. S1d) become more symmetric and centred around zero.

These results highlight the importance of bias correction as a critical pre-processing step to reduce systematic errors and improve the quality of inputs for blending.

https://doi.org/10.5194/egusphere-2026-666
Preprint. Discussion started: 5 February 2026

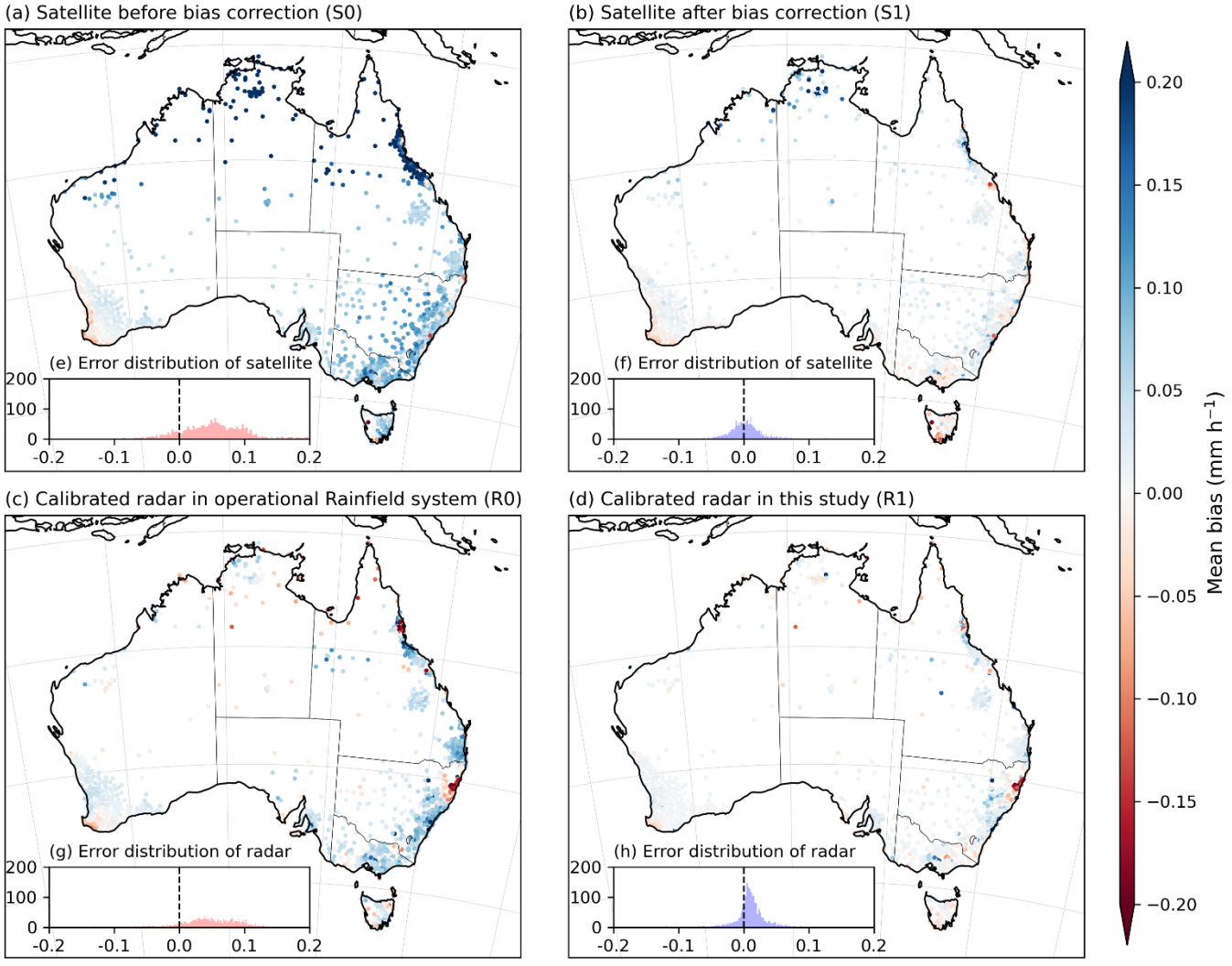

Figure 3. Spatial distribution of mean bias error (mm/h) for (a, b) satellite precipitation before (S0) and after (S1) bias correction, and (c, d) radar precipitation calibrated using the operational Rainfields system (R0) and the method in this study (R1). The Rainfields system calibration (R0) utilizes sub-daily gauges within a 150-km radius and a 15-min time window, whereas the calibration in this study (R1) is expanded to a 300-km radius and a 1-hour time window. The analysis includes all available hourly gauges from 2022 to 2023. Histograms illustrate the error distributions across all hourly gauges for the corresponding datasets, with the dashed line marking zero bias. Note that the number of gauges in satellite plots differs from radar plots because gauges outside the radar coverage are excluded from the radar analysis. An extended analysis in different subregions is provided in Fig. S1.

https://doi.org/10.5194/egusphere-2026-666
Preprint. Discussion started: 5 February 2026

4.2 Error characterisation

Figure 4 presents a subregion-dependent analysis of error variance and error correlation for satellite and radar products. Figure 4a shows that error variance increases quadratically with precipitation intensity for both products. Satellite data have higher variance than radar across all intensities, especially in tropical regions, where the fitted curve is steepest. Radar consistently shows lower error variance, reflecting its generally higher accuracy and justifying its greater weighting in blending. The constant term of the quadratic fit was fixed to ensure an approximate 2:1 error ratio between satellite and radar. To account for gauge errors, the error variance of a gauge was defined as the precipitation intensity plus one. This was based on empirical estimates from Xie and Xiong (2011), due to the limited availability of sub-daily gauge data in Australia. Figure 4b shows that satellite error correlation declines exponentially with distance, consistent across all subregions. Tropical areas exhibit the highest short-range correlations, followed by subtropical and temperate zones. Only satellite error correlations are shown, as radar–radar and radar–gauge correlations were not considered. These results highlight region-specific error characteristics. The quadratic relationship with intensity underscores the need for intensity-dependent error handling, while the exponential decay in correlation reflects the spatially localised nature of precipitation errors.

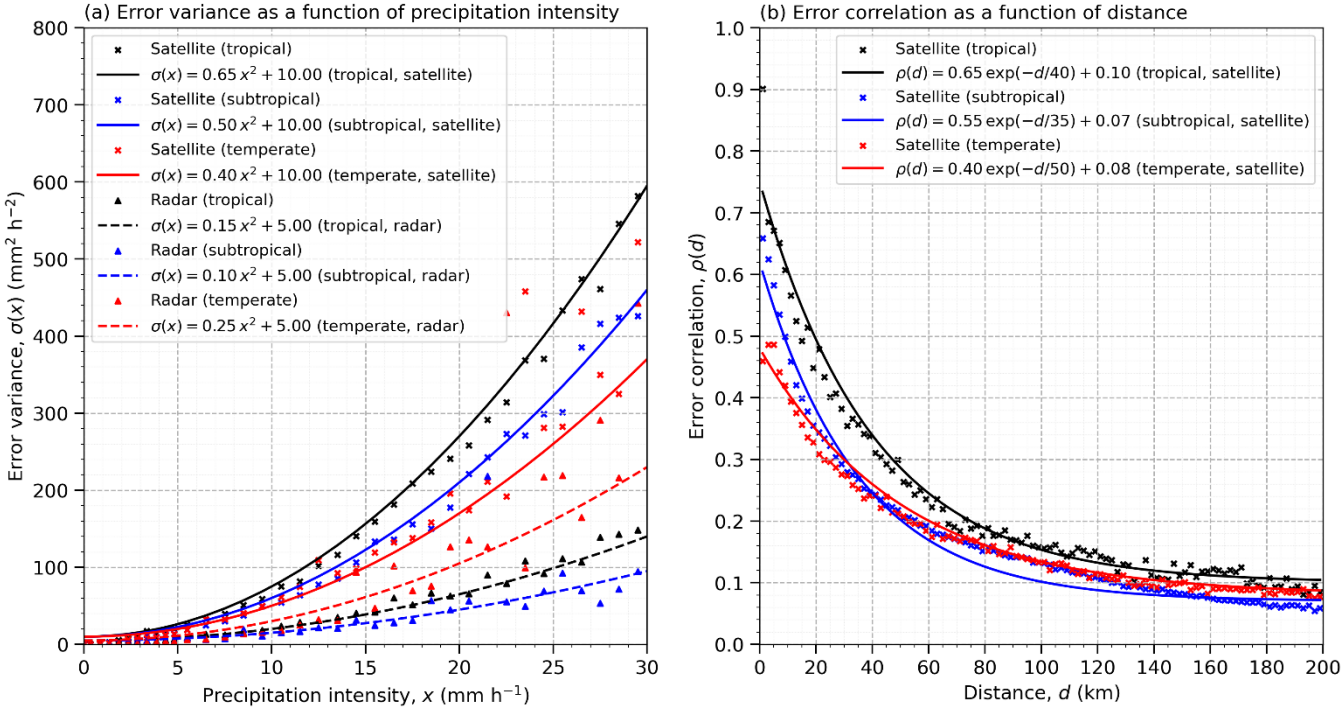

Figure 4. (a) Error variance as a function of precipitation intensity for satellite and radar precipitation products across tropical, subtropical, and temperate regions. Quadratic functions are fitted to the data for each region and dataset. (b) Error correlation as a function of distance for satellite precipitation products in the same regions, with exponential decay functions fitted to the data. These results highlight the dependency of error variance on precipitation intensity and the spatial structure

https://doi.org/10.5194/egusphere-2026-666
Preprint. Discussion started: 5 February 2026

of error correlation across climatic zones. The radar error variance in different zones does not fully reflect the spatial characteristics of individual radars, as their errors are more radar-specific. For simplicity, we grouped radars within the same subregions and derived the error variance curves accordingly.

4.3 Evaluation

4.3.1 Comparison of blended product and individual data sources

To evaluate the effectiveness of the blended product (BR-SRG; BRAIN with satellite-radar-gauge blending), we compared it against its input sources (satellite, radar and gauge) under a consistent framework. Two validation approaches were used: (1) cross-validation using hourly gauges, where the target gauges were excluded from the blending process, and (2) additional evaluation using daily gauges not involved in the blending. These evaluations covered both radar-covered and non-radar regions (Figs. 5–6; spatial maps in Figs. S5–S10). The boxplots summarise the distribution of performance metrics using both the median and interquartile range, providing a robust comparison across data sources and products.

https://doi.org/10.5194/egusphere-2026-666
Preprint. Discussion started: 5 February 2026

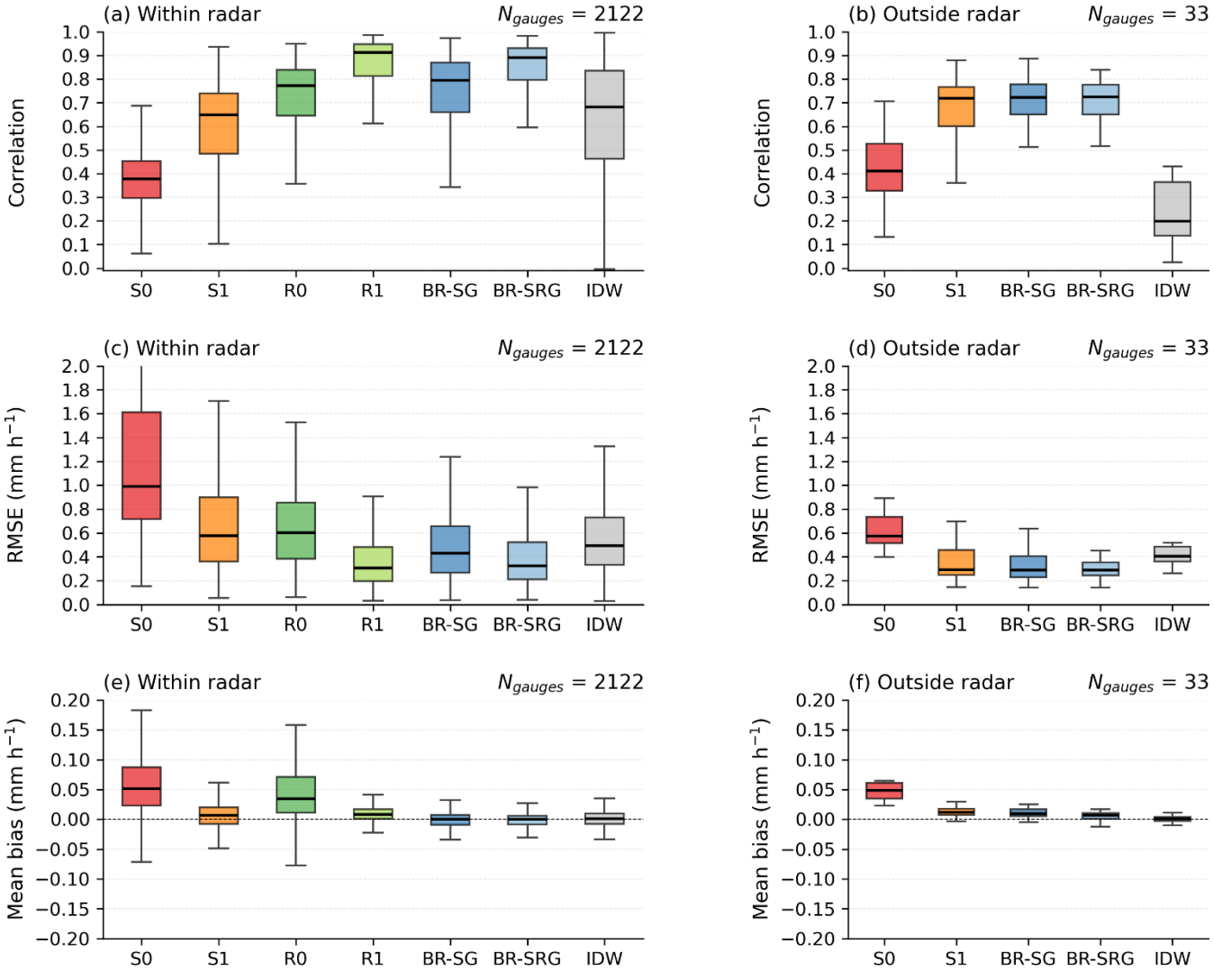

Figure 5. Combined 20-fold cross-validation for different products evaluated against hourly gauges, separated by location: (a, c, e) within radar range and (b, d, f) outside radar range (see Fig. 1a). Panels show correlation (a, b), RMSE (c, d), and mean bias (e, f). Higher correlation, lower RMSE, and bias closer to zero indicate better performance. Products include raw satellite (S0), bias-corrected satellite (S1), original radar (R0), bias-corrected radar (R1), two-source blend (BR-SG; BRAIN with satellite and gauge), three-source blend (BR-SRG; BRAIN with satellite radar and gauge), and gauge-based interpolation (IDW). In each fold, hourly gauges for evaluation were selected without replacement.

https://doi.org/10.5194/egusphere-2026-666
Preprint. Discussion started: 5 February 2026

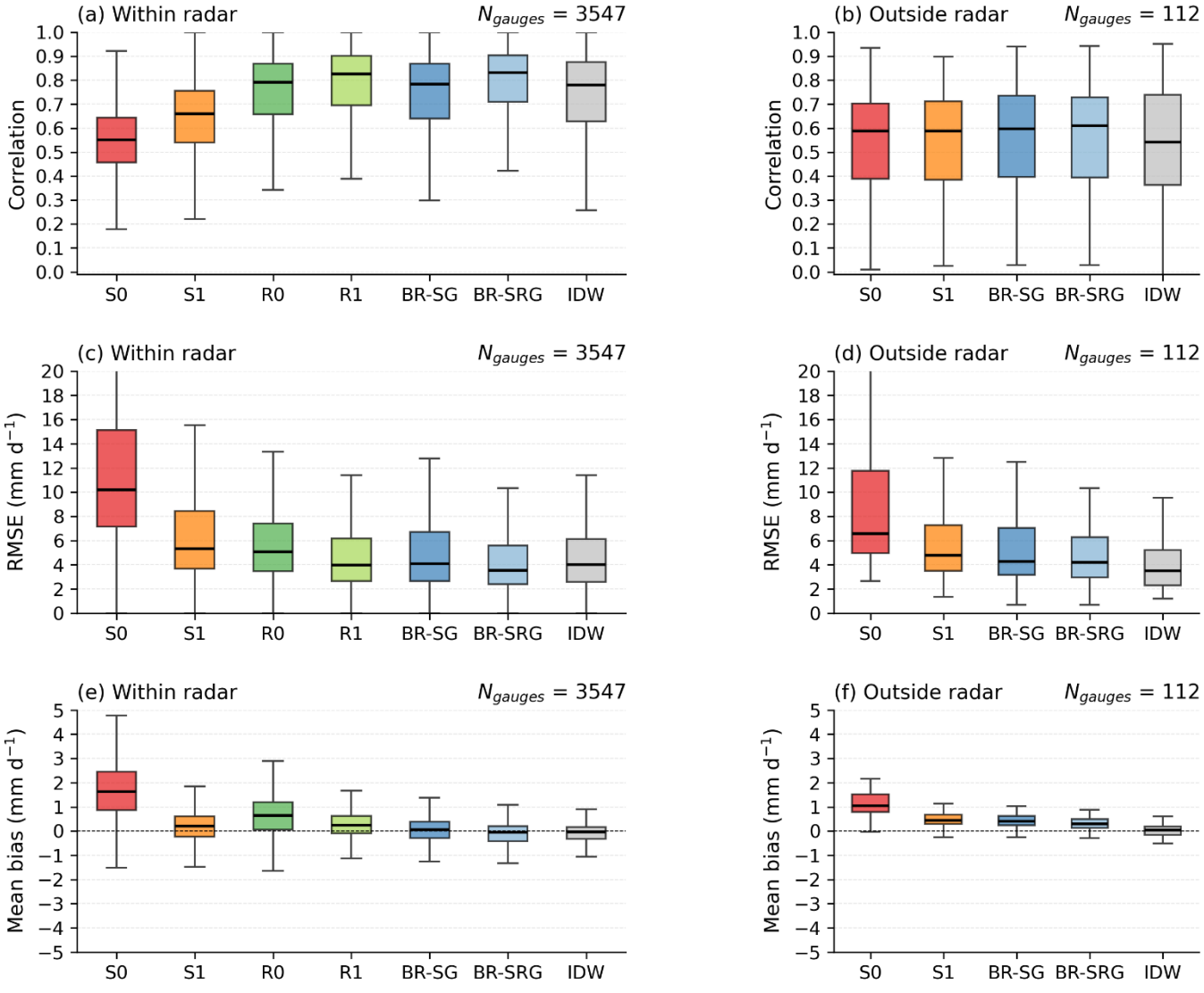

Figure 6. Evaluation using daily gauges for different products: (a, c, e) within radar range and (b, d, f) outside radar range (see Fig. 1b). Panels show correlation (a, b), RMSE (c, d), and mean bias (e, f). Higher correlation, lower RMSE, and bias closer to zero indicate better performance. Products include raw satellite (S0), bias-corrected satellite (S1), original radar (R0), bias-corrected radar (R1), two-source blend (BR-SG; BRAIN with satellite and gauge), three-source blend (BR-SRG; BRAIN with satellite radar and gauge), and gauge-based interpolation (IDW).

Compared with satellite-only products, BR-SRG (BRAIN with satellite, radar and gauge) consistently outperforms both the raw satellite estimates (S0) and the bias-corrected satellite product (S1) across both hourly and daily evaluations. Improvements are evident across all three metrics. In terms of correlation, BR-SRG exhibits higher median values than S0 and S1, indicating a stronger agreement with gauge observations. RMSE is also substantially reduced, reflecting improved

https://doi.org/10.5194/egusphere-2026-666
Preprint. Discussion started: 5 February 2026

accuracy in representing rainfall magnitude. In addition, BR-SRG shows markedly reduced mean bias, with median values closer to zero and a narrower interquartile range, indicating improved bias control and more consistent performance across gauges. These performance gains are observed both within radar-covered regions and outside radar range, demonstrating that the benefits of multi-source blending extend beyond areas directly observed by radar. This highlights the added value of integrating radar and gauge observations with satellite estimates within the statistical interpolation framework, improving both spatial representativeness and quantitative accuracy. Although bias correction improves S1 relative to S0, the satellite-only products remain clearly inferior to the multi-source blended analyses across all metrics and temporal scales.

Compared with radar-based products, within radar-covered regions, the bias corrected radar product (R1) exhibits hourly performance that is comparable to, and in some cases slightly better than, BR-SRG in terms of correlation and RMSE (Fig. 5). This behaviour is expected, as R1 is calibrated using more available gauges, which favours performance at hourly timescales within radar coverage. When evaluated using additional daily gauge observations, BR-SRG consistently outperforms R1 in both correlation and RMSE (Fig. 6), indicating improved robustness and reduced sensitivity to radar-specific errors. This improvement is also reflected in the mean bias statistics at both hourly and daily evaluations, where BR-SRG shows median values closer to zero and a narrower interquartile range than R1, suggesting more stable bias control across gauges. Outside radar coverage, radar-based observations are not applicable, whereas BR-SRG maintains stable performance by leveraging satellite, radar and gauge information through spatial proximity, further highlighting the advantage of the multi-source blending framework.

Compared with the current operational gauge-based IDW method, BR-SRG shows consistently better performance in both hourly and daily evaluations (Figs. 5–6), particularly within radar-covered regions. Outside the radar range, BR-SRG continues to achieve higher correlation but exhibits higher daily RMSE than IDW. Several factors help explain this behaviour. First, sub-daily rainfall exhibits short error correlation length scales (see Fig. 4b), which restrict the spatial influence of gauge observations within the statistical interpolation framework. As a result, BR-SRG increasingly relies on satellite estimates as the distance from gauges grows. In contrast, IDW always incorporates gauge observations regardless of distance and can extract some information even from distant stations (see Fig. S3 and Text S2b). Second, the availability of sub-daily gauge observations decreases substantially with distance, especially outside the radar coverage, reducing the effectiveness of satellite calibration. As a result, residual satellite biases may propagate into the blended product (see Fig. S9a and Fig. S10a). Because BR-SRG increasingly depends on satellite information in these regions, such residual biases can adversely affect performance (see Fig. 1a, Fig. S2, and Text S2a). Third, IDW may benefit from partial error cancellation when sub-daily estimates are aggregated to daily values, which can lead to lower daily RMSE despite weaker sub-daily performance (see Fig. 6f and Fig. S10c). It is also important to note that the evaluation outside radar coverage is constrained by the sparse availability of daily gauge observations. Nevertheless, IDW consistently underperforms BR-SRG within radar-covered areas and is markedly less effective at representing spatial rainfall structure (Fig. 7), underscoring the overall advantage of the multi-source blended approach.

https://doi.org/10.5194/egusphere-2026-666
Preprint. Discussion started: 5 February 2026

Overall, BR-SRG outperforms each individual data source by effectively combining satellite, radar, and gauge observations. It performs best within radar coverage and remains competitive outside. The performance outside radar range is largely influenced by satellite quality, suggesting the need to further improve both satellite retrieval algorithms and calibration methods.

An additional independent hourly dataset (~2000 gauges) was collated after completion of the main analyses and used for supplementary evaluation (Fig. S14), and the results strongly reinforce the finding that the blended product (BR-SRG) exhibits superior overall performance compared with satellite, radar, and gauge products.

4.3.2 Comparison of three-source and two-source blending

The three-source blended product (BR-SRG; satellite–radar–gauge) was also compared with the two-source combination (BR-SG; satellite–gauge) using both hourly cross-validation and additional daily validation (Figs. 5–6). Across both temporal scales, BR-SRG consistently outperforms BR-SG both within and beyond radar coverage, demonstrating the added value of incorporating radar observations into the blending framework.

Within radar-covered regions, the inclusion of radar data leads to clear improvements in both correlation and RMSE at the hourly scale, reflecting the ability of radar to capture fine-scale spatial and temporal rainfall variability that cannot be resolved by satellite and gauge data alone. These improvements persist, albeit to a lesser extent, in the daily evaluation, indicating that the benefits of radar assimilation extend beyond short-term variability and contribute to improved accumulation accuracy. The reduction in mean bias and interquartile range further suggests that radar data help stabilise the blended estimates across gauges.

Beyond radar coverage, BR-SRG continues to show modest but consistent improvements over BR-SG. Although radar observations are not directly available in these regions, their influence propagates through the statistical interpolation framework over short distances, particularly near the radar boundary. This short-range extrapolation allows radar information to indirectly constrain the blended field, leading to improved performance relative to the two-source configuration. The magnitude of these gains decreases with distance from radar coverage, consistent with the short spatial correlation length scales of sub-daily precipitation errors.

Overall, the comparison between BR-SRG and BR-SG confirms that radar observations provide complementary information to satellite and gauge data, enhancing both the accuracy and robustness of blended precipitation estimates. These results highlight the importance of retaining radar data within national-scale blending systems where available, while also demonstrating that the multi-source framework remains effective under heterogeneous observational coverage, a key requirement for operational applications.

https://doi.org/10.5194/egusphere-2026-666
Preprint. Discussion started: 5 February 2026

4.3.3 Comparison of hourly blended product and daily operational product

Figure 7 (with further details in Fig. S4 and Tables S1 and S2) compares the hourly blended product (BR-SRG) with the AGCD daily product and hourly gauge-based IDW interpolation for two extreme precipitation events: 24 December 2022 and 14 December 2023. While all products capture large-scale rainfall patterns, BR-SRG clearly outperforms AGCD and IDW in representing fine-scale spatial structure and intensity.

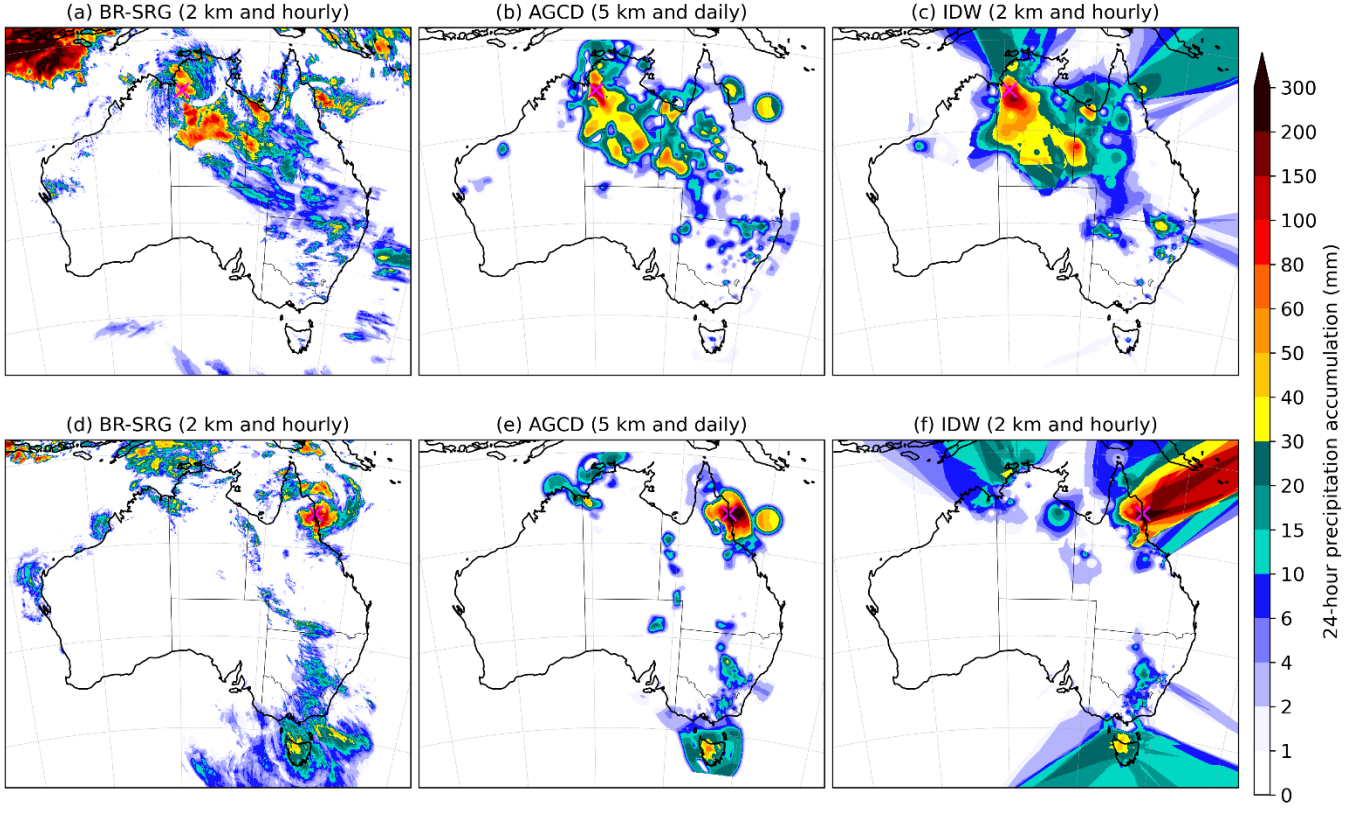

Figure 7. Comparison of the blended product (BR-SRG; 2-km and hourly), the AGCD product (5-km and daily), and the gauge-based IDW interpolation (2-km and hourly) for two extreme precipitation events: (a–c) 24-hour accumulation on 24 December 2022 and (d–f) 24-hour accumulation on 14 December 2023. BR-SRG is derived from hourly data accumulated over 9 am–9 am local time, while AGCD is a daily gauge-based product, and IDW is derived from sub-daily gauge interpolation. The "×" symbol marks the gauge location with the highest observed precipitation for each event. For the 24 December 2022 event, the observed gauge totals are 168.2 mm (from hourly gauges) and 208.0 mm (from daily gauges). Corresponding values in each product are: 110.8 mm in BR-SRG (a), 175.8 mm in AGCD (b), and 132.5 mm in IDW (c). For the 14 December 2023 event, the observed gauge totals are 479.2 mm (from hourly gauges) and 572.4 mm (from daily gauges). Corresponding values in each product are: 456.3 mm in BR-SRG (d), 410.6 mm in AGCD (e), and 261.3 mm in IDW (f). Further details are provided in Fig. S4 and Tables S1 and S2.

https://doi.org/10.5194/egusphere-2026-666
Preprint. Discussion started: 5 February 2026

For the 24 December 2022 event, BR-SRG (Fig. 7a) shows localised high-intensity rainfall across northern Australia, while IDW (Fig. 7c) underestimates peaks and lacks spatial detail. AGCD (Fig. 7b) captures the maximum rainfall centre reasonably well due to the availability of multiple daily gauges (Fig. S4b and Table S1) in the area but it is too smooth due to not processing enough fine-scale information. For the 14 December 2023 event, BR-SRG (Fig. 7d) again provides a detailed representation of extreme rainfall patterns in northern and southeastern Australia, supported by a denser sub-daily gauge network (Fig. S4c and Table S2). AGCD (Fig. 7e) fails to capture the peak at Cape Tribulation, likely due to delayed or excluded gauge data (Fig. S4d and Table S2). IDW (Fig. 7f) reproduces the general pattern but underestimates intensity. These results highlight the strength and added value of BR-SRG in generating high-resolution hourly fields that preserve the spatial detail of extreme events, reinforcing its operational potential. Incorporating daily gauges could further improve performance, though this must be balanced against the timeliness required for near-real-time applications.

4.4 Spatial and temporal performance of the blended product

Figure 8 shows the spatial performance of the blended product (BR-SRG) using correlation and RMSE metrics against hourly gauge observations. High correlations are observed across most regions, particularly where gauge density is higher (Fig. 8a–c). RMSE is generally lower in coastal and well-observed areas, with higher values in regions with sparse gauges or greater rainfall variability (Fig. 8d–f). Some outliers may result from imperfect gauge quality control or residual errors in satellite and radar inputs (see Fig. S6). Evaluation may also be biased at gauges with limited data, such as those operating only during wet seasons. Additional assessments of daily spatial performance (Fig. S11) and monthly temporal performance at both hourly and daily scales (Fig. S12) are provided in the Supplementary Material. Overall, BR-SRG performs strongly across Australia, with room for improvement in sparsely gauged regions.

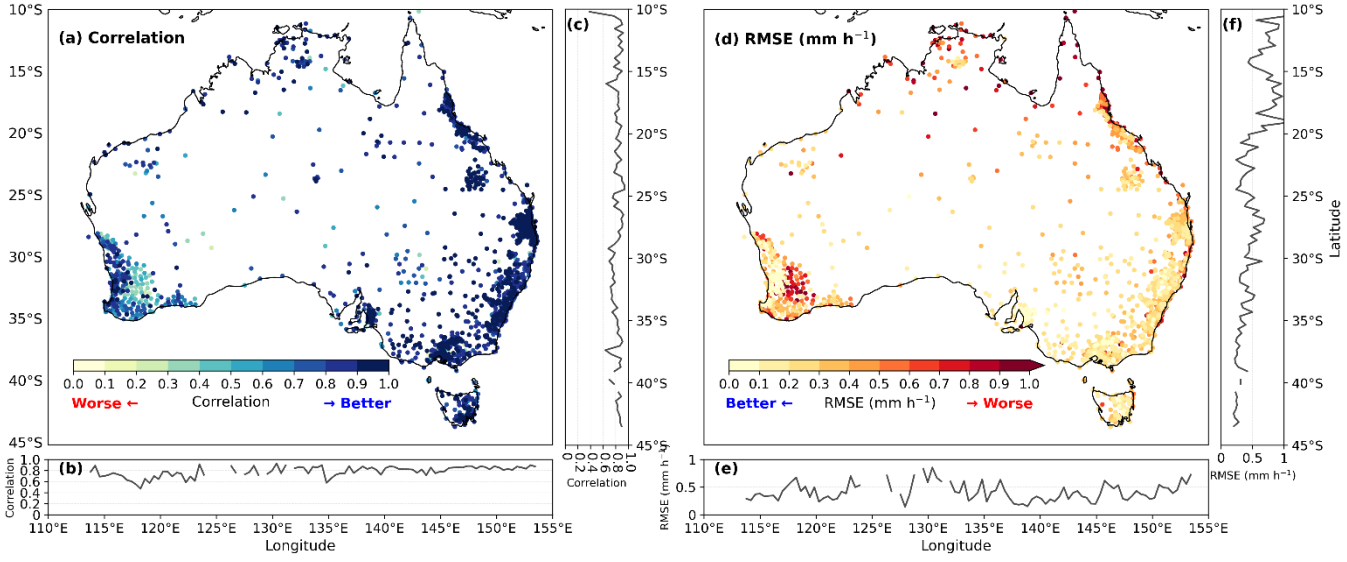

https://doi.org/10.5194/egusphere-2026-666
Preprint. Discussion started: 5 February 2026

Figure 8. Spatial performance of the blended product (BR-SRG) on hourly gauges across Australia. (a) Spatial distribution of correlation between BR-SRG and hourly gauge observations, with higher values (blue) indicating better performance. (d) Spatial distribution of RMSE (mm/h), with lower values (red) indicating better performance. (b, e) Longitudinal variations of (b) correlation and (e) RMSE averaged across gauges. (c, f) Latitudinal variations of (c) correlation and (f) RMSE averaged across gauges.

5 Conclusions and future directions

In this study, we developed and trialled BRAIN, a national-scale multi-source precipitation analysis system that blends Himawari satellite rainfall estimates, Rainfields radar products, and hourly gauge observations to generate a 2-km, hourly gridded rainfall dataset for Australia. The system addresses a long-standing need for high-resolution, sub-daily rainfall information by combining methodological rigor with computational scalability under realistic operational constraints. Comprehensive evaluation over a two-year trial period (2022–2023) demonstrates that the blended product consistently outperforms individual data sources, two-source blending configurations, and the operational gauge-based IDW approach, while producing spatially coherent and quantitatively consistent rainfall fields suitable for both historical analysis and near–real-time applications.

The key conclusions of this study can be summarised as follows:

(1) The high-frequency Himawari CRRPH product is demonstrated to be an effective background field for national-scale precipitation blending. Its key role is to provide a spatially complete first guess at very high spatial and temporal resolution, onto which higher-accuracy radar and gauge observations can be consistently integrated where available. In regions where ground-based observations are sparse or absent, the satellite background effectively fills spatial gaps, ensuring continuity and stability of the blended rainfall field across the continent.

(2) The continental-scale trial implementation successfully integrates all currently available and operationally manageable observation-based data sources in Australia, including satellite, radar, and gauge observations, within a unified statistical framework. The system is already under active testing within the Bureau's internal environment and is technically ready for operationalisation. In the longer term, the framework is designed to support both historical reconstruction and near–real-time product generation, providing a consistent and flexible rainfall analysis capability for a wide range of users.

(3) The error-informed localisation strategy embedded within the statistical interpolation framework is shown to be effective at continental scale. In particular, the nearest-point approximation for gridded radar source substantially reduces modelling and computational complexity, enabling multi-source blending at kilometre and hourly resolutions over large spatial domains. This strategy preserves the dominant information content of each data source while making high-resolution, sub-daily national analyses computationally feasible.

https://doi.org/10.5194/egusphere-2026-666
Preprint. Discussion started: 5 February 2026

(4) The added value of the blended product is confirmed through comprehensive comparisons against individual data sources, alternative blending configurations, and existing operational methods and products. The blended analyses consistently outperform single-source fields and two-source blending approaches and exhibit strong spatial and quantitative consistency with the daily operational AGCD product, supporting their reliability for both sub-daily and aggregated applications.

Future development of BRAIN will focus on improving input data quality, refining error characterisation, and enhancing spatial and temporal resolution. Anticipated upgrades to the Himawari-based CRRPH product are expected to further improve performance, particularly in tropical and radar-sparse regions, while ongoing radar recalibration efforts are likely to enhance local accuracy. The integration of complementary satellite products (e.g. IMERG), additional ground-based observations (including daily gauges and third-party sub-daily data), and improved representation of error characteristics in sparsely observed regions will further strengthen the system.

Overall, BRAIN represents an important step towards an operational national sub-daily rainfall analysis capability for Australia. Beyond its immediate regional relevance, this study provides an additional reference for large-scale multi-source precipitation analysis systems at kilometre and hourly resolutions under heterogeneous observational conditions.

Data availability

The Himawari CRRPH satellite precipitation data can be accessed via the National Computational Infrastructure (NCI) Data Catalogue (https://dx.doi.org/10.25914/qc2q-mx21). Radar precipitation data are also available through the NCI Data Catalogue (https://dx.doi.org/10.25914/5cb686a8d9450). The BRAIN product is currently on pre-production test and working to allow its transition into production. Other datasets that are not openly accessible can be requested from the Australian Bureau of Meteorology.

Author contributions

YZ developed the methodology, performed the formal analysis, implemented the software, carried out the validation and visualization, and prepared the original draft of the manuscript. QW, AF, JP, BT, and CV contributed to the conceptualization, investigation, methodology, formal analysis, and validation of the study. AF, JP, BT, CV, and VV curated the datasets used in the analysis. QW, AF, and CV were responsible for funding acquisition, project administration, and supervision. AF and CV provided key resources supporting the study. CS contributed to the formal analysis, methodology, investigation, and validation. All authors contributed to manuscript review and editing and approved the final version.

Competing interests

The authors declare that they have no conflict of interest.

https://doi.org/10.5194/egusphere-2026-666
Preprint. Discussion started: 5 February 2026

Disclaimer

Copernicus Publications remains neutral with regard to jurisdictional claims made in the text, published maps, institutional affiliations, or any other geographical representation in this paper. While Copernicus Publications makes every effort to include appropriate place names, the final responsibility lies with the authors. Views expressed in the text are those of the authors and do not necessarily reflect the views of the publisher.

Acknowledgements

We sincerely thank Bureau of Meteorology's scientists Dr. Zhi-Weng Chua, Dr. Caroline Poulsen for their valuable feedback during the internal review process of this manuscript. We also thank Dr. Mahadi Hasan for his assistance in processing the additional hourly gauge dataset and the Bureau's flood and data teams for support supplying that data. We gratefully acknowledge the numerous organisations and agencies across the Australian water sector for their contributions of flood and water information to the Bureau of Meteorology under the Water Act 2007. This research was undertaken with the assistance of resources and services provided by the National Computational Infrastructure (NCI Australia), which is supported by the Australian Government. This research has been funded by the Bureau of Meteorology as part of the Next Generation Rainfall Project.

References

Acharya, S. C., Nathan, R., Wang, Q. J., and Su, C.-H.: Temporal disaggregation of daily rainfall measurements using regional reanalysis for hydrological applications, Journal of Hydrology, 610, 127867, https://doi.org/10.1016/j.jhydrol.2022.127867, 2022.

Beck, H. E., van Dijk, A. I. J. M., Levizzani, V., Schellekens, J., Miralles, D. G., Martens, B., and de Roo, A.: MSWEP: 3-hourly 0.25deg, global gridded precipitation (1979-2015) by merging gauge, satellite, and reanalysis data, Hydrology and Earth System Sciences, 21, 589–615, https://doi.org/10.5194/hess-21-589-2017, 2017.

Beck, H. E., Wood, E. F., Pan, M., Fisher, C. K., Miralles, D. G., Dijk, A. I. J. M. van, McVicar, T. R., and Adler, R. F.: MSWEP V2 Global 3-Hourly 0.1° Precipitation: Methodology and Quantitative Assessment, Bulletin of the American Meteorological Society, 100, 473–500, https://doi.org/10.1175/BAMS-D-17-0138.1, 2019.

Bergman, K. H.: Role of Observational Errors in Optimum Interpolation Analysis, Bulletin of the American Meteorological Society, 59, 1603–1611, https://doi.org/10.1175/1520-0477-59.12.1603, 1978.

Bhargava, M. and Danard, M.: Application of Optimum Interpolation to the Analysis of Precipitation in Complex Terrain, Journal of Applied Meteorology and Climatology, 33, 508–518, https://doi.org/10.1175/1520-0450(1994)033<0508:AOOITT>2.0.CO;2, 1994.

Bureau of Meteorology: AURA - Operational Radar Network Archive, https://dx.doi.org/10.25914/5cb686a8d9450, 2022.

Bureau of Meteorology: Himawari 8/9 - Convective Rain Rate - Physically Based (CRRPH) (V2.1), https://dx.doi.org/10.25914/qc2q-mx21, 2024.

https://doi.org/10.5194/egusphere-2026-666
Preprint. Discussion started: 5 February 2026

Bureau of Meteorology: Australia Rainfall and River Conditions, 2025.

Chappell, A., Renzullo, L. J., Raupach, T. H., and Haylock, M.: Evaluating geostatistical methods of blending satellite and gauge data to estimate near real-time daily rainfall for Australia, Journal of Hydrology, 493, 105–114, https://doi.org/10.1016/j.jhydrol.2013.04.024, 2013.

Chua, Z.-W., Kuleshov, Y., Watkins, A. B., Choy, S., and Sun, C.: A Two-Step Approach to Blending GSMaP Satellite Rainfall Estimates with Gauge Observations over Australia, Remote Sensing, 14, 1903, https://doi.org/10.3390/rs14081903, 2022a.

Chua, Z.-W., Kuleshov, Y., Watkins, A. B., Choy, S., and Sun, C.: A Two-Step Approach to Blending GSMaP Satellite Rainfall Estimates with Gauge Observations over Australia, Remote Sensing, 14, 1903, https://doi.org/10.3390/rs14081903, 2022b.

Chua, Z.-W., Evans, A., Kuleshov, Y., Watkins, A., Choy, S., and Sun, C.: Enhancing the Australian Gridded Climate Dataset rainfall analysis using satellite data, Sci Rep, 12, 20691, https://doi.org/10.1038/s41598-022-25255-6, 2022c.

Chua, Z.-W., Kuleshov, Y., Watkins, A. B., Choy, S., and Sun, C.: A Statistical Interpolation of Satellite Data with Rain Gauge Data over Papua New Guinea, Journal of Hydrometeorology, 24, 2369–2387, https://doi.org/10.1175/JHM-D-23-0035.1, 2023.

Chumchean, S., Seed, A., and Sharma, A.: Correcting of real-time radar rainfall bias using a Kalman filtering approach, Journal of Hydrology, 317, 123–137, https://doi.org/10.1016/j.jhydrol.2005.05.013, 2006.

De Mey, P.: Optimal Interpolation in a model of the Azores Current in 1986–88, in: Data Assimilation, Berlin, Heidelberg, 85–105, https://doi.org/10.1007/978-3-642-78939-7_4, 1994.

Dong, J., Crow, W. T., Chen, X., Tangdamrongsub, N., Gao, M., Sun, S., Qiu, J., Wei, L., Gao, H., and Duan, Z.: Statistical uncertainty analysis-based precipitation merging (SUPER): A new framework for improved global precipitation estimation, Remote Sensing of Environment, 283, 113299, https://doi.org/10.1016/j.rse.2022.113299, 2022.

Evans, A., Jones, D., Smalley, R., and Lellyett, S.: An enhanced gridded rainfall analysis scheme for Australia, BoM report, 2020.

Fortin, V., Roy, G., Donaldson, N., and Mahidjiba, A.: Assimilation of radar quantitative precipitation estimations in the Canadian Precipitation Analysis (CaPA), Journal of Hydrology, 531, 296–307, https://doi.org/10.1016/j.jhydrol.2015.08.003, 2015.

Fortin, V., Roy, G., Stadnyk, T., Koenig, K., Gasset, N., and Mahidjiba, A.: Ten Years of Science Based on the Canadian Precipitation Analysis: A CaPA System Overview and Literature Review, Atmosphere-Ocean, 56, 178–196, https://doi.org/10.1080/07055900.2018.1474728, 2018.

Gandin, L.: Objective analysis of meteorological fields, Israel Program for Scientific Translations, 242, 1963.

Gauthier, P., Tanguay, M., Laroche, S., Pellerin, S., and Morneau, J.: Extension of 3DVAR to 4DVAR: Implementation of 4DVAR at the Meteorological Service of Canada, Monthly Weather Review, 135, 2339–2354, https://doi.org/10.1175/MWR3394.1, 2007.

https://doi.org/10.5194/egusphere-2026-666
Preprint. Discussion started: 5 February 2026

Gavahi, K., Foroumandi, E., and Moradkhani, H.: A deep learning-based framework for multi-source precipitation fusion, Remote Sensing of Environment, 295, 113723, https://doi.org/10.1016/j.rse.2023.113723, 2023.

Huang, X.-Y., Gustafsson, N., and Källén, E. R.: Using an adjoint model to improve an optimum interpolation-based data-assimilation system, Tellus A, 49, 161–176, https://doi.org/10.1034/j.1600-0870.1997.t01-1-00001.x, 1997.

Hyfte, S. V., Moigne, P. L., Bazile, E., Verrelle, A., and Boone, A.: High-Resolution Reanalysis of Daily Precipitation using AROME Model Over France, Tellus A, 75, 27–49, https://doi.org/10.16993/tellusa.95, 2023.

Imhoff, R. O., De Cruz, L., Dewettinck, W., Brauer, C. C., Uijlenhoet, R., van Heeringen, K.-J., Velasco-Forero, C., Nerini, D., Van Ginderachter, M., and Weerts, A. H.: Scale-dependent blending of ensemble rainfall nowcasts and numerical weather prediction in the open-source pysteps library, Quarterly Journal of the Royal Meteorological Society, 149, 1335–1364, https://doi.org/10.1002/qj.4461, 2023.

Islam, Md. A., Yu, B., and Cartwright, N.: Assessment and comparison of five satellite precipitation products in Australia, Journal of Hydrology, 590, 125474, https://doi.org/10.1016/j.jhydrol.2020.125474, 2020.

Jeffrey, S. J., Carter, J. O., Moodie, K. B., and Beswick, A. R.: Using spatial interpolation to construct a comprehensive archive of Australian climate data, Environmental Modelling & Software, 16, 309–330, https://doi.org/10.1016/S1364-8152(01)00008-1, 2001.

Jones, D., Wang, W., and Fawcett, R.: High-quality spatial climate data-sets for Australia, AMOJ, 58, 233–248, https://doi.org/10.22499/2.5804.003, 2009.

Khedhaouiria, D., Bélair, S., Fortin, V., Roy, G., and Lespinas, F.: High-Resolution (2.5 km) Ensemble Precipitation Analysis across Canada, Journal of Hydrometeorology, 21, 2023–2039, https://doi.org/10.1175/JHM-D-19-0282.1, 2020.

Khedhaouiria, D., Bélair, S., Fortin, V., Roy, G., and Lespinas, F.: Using a hybrid optimal interpolation–ensemble Kalman filter for the Canadian Precipitation Analysis, Nonlinear Processes in Geophysics, 29, 329–344, https://doi.org/10.5194/npg-29-329-2022, 2022a.

Khedhaouiria, D., Bélair, S., Fortin, V., Roy, G., and Lespinas, F.: Using a hybrid optimal interpolation–ensemble Kalman filter for the Canadian Precipitation Analysis, Nonlin. Processes Geophys., 29, 329–344, https://doi.org/10.5194/npg-29-329-2022, 2022b.

Kossieris, P., Tsoukalas, I., Brocca, L., Mosaffa, H., Makropoulos, C., and Anghelea, A.: Precipitation data merging via machine learning: Revisiting conceptual and technical aspects, Journal of Hydrology, 637, 131424, https://doi.org/10.1016/j.jhydrol.2024.131424, 2024.

Koster, R. D., Liu, Q., Reichle, R. H., and Huffman, G. J.: Improved Estimates of Pentad Precipitation Through the Merging of Independent Precipitation Data Sets, Water Resources Research, 57, e2021WR030330, https://doi.org/10.1029/2021WR030330, 2021.

Lorenc, A. C., Bell, R. S., and Macpherson, B.: The Meteorological Office analysis correction data assimilation scheme, Quarterly Journal of the Royal Meteorological Society, 117, 59–89, https://doi.org/10.1002/qj.49711749704, 1991.

Ma, Z., Xu, J., Dong, B., Hu, X., Hu, H., Yan, S., Zhu, S., He, K., Shi, Z., Chen, Y., Fang, X., Zhang, Q., Gu, S., and Weng, F.: GMCP: A Fully Global Multisource Merging-and-Calibration Precipitation Dataset (1-Hourly, 0.1°, Global, 2000–the

https://doi.org/10.5194/egusphere-2026-666
Preprint. Discussion started: 5 February 2026

Present), Bulletin of the American Meteorological Society, 106, E596–E624, https://doi.org/10.1175/BAMS-D-24-0051.1, 2025.

Mahfouf, J., Brasnett, B., and Gagnon, S.: A Canadian precipitation analysis (CaPA) project: Description and preliminary results, Atmosphere-Ocean, 45, 1–17, https://doi.org/10.3137/ao.v450101, 2007.

Mitchell, H. L., Charette, C., Chouinard, C., and Brasnett, B.: Revised Interpolation Statistics for the Canadian Data Assimilation Procedure: Their Derivation and Application, Monthly Weather Review, 118, 1591–1614, https://doi.org/10.1175/1520-0493(1990)118<1591:RISFTC>2.0.CO;2, 1990.

Nishant, N., Sherwood, S., Prasad, A., Ji, F., and Singh, A.: Impact of Higher Spatial Resolution on Precipitation Properties Over Australia, Geophysical Research Letters, 49, e2022GL100717, https://doi.org/10.1029/2022GL100717, 2022.

Prein, A. F., Rasmussen, R. M., Ikeda, K., Liu, C., Clark, M. P., and Holland, G. J.: The future intensification of hourly precipitation extremes, Nature Climate Change, 7, 48–52, https://doi.org/10.1038/nclimate3168, 2017.

Rabier, F.: Overview of global data assimilation developments in numerical weather-prediction centres, Quarterly Journal of the Royal Meteorological Society, 131, 3215–3233, https://doi.org/10.1256/qj.05.129, 2005.

Rabier, F., Järvinen, H., Klinker, E., Mahfouf, J.-F., and Simmons, A.: The ECMWF operational implementation of four-dimensional variational assimilation. I: Experimental results with simplified physics, Quarterly Journal of the Royal Meteorological Society, 126, 1143–1170, https://doi.org/10.1002/qj.49712656415, 2000.

Rawlins, F., Ballard, S. P., Bovis, K. J., Clayton, A. M., Li, D., Inverarity, G. W., Lorenc, A. C., and Payne, T. J.: The Met Office global four-dimensional variational data assimilation scheme, Quarterly Journal of the Royal Meteorological Society, 133, 347–362, https://doi.org/10.1002/qj.32, 2007.

Renzullo, L. J., Velasco-Forero, C. A., and Seed, A. W.: Blending radar, NWP and satellite data for real-time ensemble rainfall analysis: a scale-dependent method, CSIRO Report, 2017.

Seed, A., Duthie, E., and Chumchean, S.: Rainfields: the Australian Bureau of Meteorology system for quantitative precipitation estimation, Proceedings 33rd AMS Conference on Radar Meteorology, Cairns, Australia, 2007.

Shen, Y., Zhao, P., Pan, Y., and Yu, J.: A high spatiotemporal gauge-satellite merged precipitation analysis over China, Journal of Geophysical Research: Atmospheres, 119, 3063–3075, https://doi.org/10.1002/2013JD020686, 2014a.

Shen, Y., Zhao, P., Pan, Y., and Yu, J.: A high spatiotemporal gauge-satellite merged precipitation analysis over China, J. Geophys. Res. Atmos., 119, 3063–3075, https://doi.org/10.1002/2013JD020686, 2014b.

Shen, Y., Hong, Z., Pan, Y., Yu, J., and Maguire, L.: China's 1 km Merged Gauge, Radar and Satellite Experimental Precipitation Dataset, Remote Sensing, 10, 264, https://doi.org/10.3390/rs10020264, 2018.

Su, C.-H., Eizenberg, N., Steinle, P., Jakob, D., Fox-Hughes, P., White, C. J., Rennie, S., Franklin, C., Dharssi, I., and Zhu, H.: BARRA v1.0: the Bureau of Meteorology Atmospheric high-resolution Regional Reanalysis for Australia, Geoscientific Model Development, 12, 2049–2068, https://doi.org/10.5194/gmd-12-2049-2019, 2019.

Su, C.-H., Eizenberg, N., Jakob, D., Fox-Hughes, P., Steinle, P., White, C. J., and Franklin, C.: BARRA v1.0: kilometre-scale downscaling of an Australian regional atmospheric reanalysis over four midlatitude domains, Geoscientific Model Development, 14, 4357–4378, https://doi.org/10.5194/gmd-14-4357-2021, 2021.

https://doi.org/10.5194/egusphere-2026-666
Preprint. Discussion started: 5 February 2026

Su, C.-H., Renie, S., Torrance, J., Howard, E., Stassen, C., Lipson, M., Warren, R. A., Pepler, A., Dharssi, I., and Franklin, C.: BARRA-C2: Development of the kilometre-scale downscaled atmospheric reanalysis over Australia, Bureau of Meteorology, 2024.

Su, C.-H., Torrance, J., Rennie, S., Howard, E., Stassen, C., Warren, R., Smith, A., Dharssi, I., Pepler, A., Tian, S., Lipson, M., Steinle, P., Franklin, C., Le, T., Wang, C., Masoumi, S., and Le Marshall, J.: The Australian regional atmospheric reanalysis system, version 2 – BARRA2, Journal of Southern Hemisphere Earth Systems Science, 75, ES25032, https://doi.org/10.1071/ES25032, 2025.

Sun, Q., Miao, C., Duan, Q., Ashouri, H., Sorooshian, S., and Hsu, K.: A Review of Global Precipitation Data Sets: Data Sources, Estimation, and Intercomparisons, Rev. Geophys., 56, 79–107, https://doi.org/10.1002/2017RG000574, 2018.

Villarini, G., Mandapaka, P. V., Krajewski, W. F., and Moore, R. J.: Rainfall and sampling uncertainties: A rain gauge perspective, Journal of Geophysical Research: Atmospheres, 113, D11102, https://doi.org/10.1029/2007JD009214, 2008.

Xie, P. and Xiong, A.-Y.: A conceptual model for constructing high-resolution gauge-satellite merged precipitation analyses, Journal of Geophysical Research: Atmospheres, 116, D21106, https://doi.org/10.1029/2011JD016118, 2011.

Xie, P., Chen, M., and Shi, W.: CPC unified gauge-based analysis of global daily precipitation, in: 24th Conference on Hydrology, 24th Conference on Hydrology, Atlanta, GA, 2010.

Xu, L., Chen, N., Moradkhani, H., Zhang, X., and Hu, C.: Improving Global Monthly and Daily Precipitation Estimation by Fusing Gauge Observations, Remote Sensing, and Reanalysis Data Sets, Water Resources Research, 56, e2019WR026444, https://doi.org/10.1029/2019WR026444, 2020.

Xu, Y., Tang, G., Li, L., and Wan, W.: Multi-source precipitation estimation using machine learning: Clarification and benchmarking, Journal of Hydrology, 635, 131195, https://doi.org/10.1016/j.jhydrol.2024.131195, 2024.

Yin, J., Guo, S., Gu, L., Zeng, Z., Liu, D., Chen, J., Shen, Y., and Xu, C.-Y.: Blending multi-satellite, atmospheric reanalysis and gauge precipitation products to facilitate hydrological modelling, Journal of Hydrology, 593, 125878, https://doi.org/10.1016/j.jhydrol.2020.125878, 2021.

Yu, J., Li, X.-F., Lewis, E., Blenkinsop, S., and Fowler, H. J.: UKGrsHP: a UK high-resolution gauge–radar–satellite merged hourly precipitation analysis dataset, Climate Dynamics, 54, 2919–2940, https://doi.org/10.1007/s00382-020-05144-2, 2020.

Zhang, W., Furtado, K., Wu, P., Zhou, T., Chadwick, R., Marzin, C., Rostron, J., and Sexton, D.: Increasing precipitation variability on daily-to-multiyear time scales in a warmer world, Science Advances, 7, eabf8021, https://doi.org/10.1126/sciadv.abf8021, 2021a.

Zhang, Y., Ye, A., Nguyen, P., Analui, B., Sorooshian, S., and Hsu, K.: Error Characteristics and Scale Dependence of Current Satellite Precipitation Estimates Products in Hydrological Modeling, Remote Sensing, 13, 3061, https://doi.org/10.3390/rs13163061, 2021b.

Zhang, Y., Ye, A., Nguyen, P., Analui, B., Sorooshian, S., and Hsu, K.: New Insights Into Error Decomposition for Precipitation Products, Geophysical Research Letters, 48, e2021GL094092, https://doi.org/10.1029/2021GL094092, 2021c.

https://doi.org/10.5194/egusphere-2026-666
Preprint. Discussion started: 5 February 2026

810 Zhang, Y., Wang, Q. J., Frost, A. J., Trewin, B., Pudashine, J., Velasco-Forero, C., Su, C.-H., and Villani, V.: Advancing High-Resolution Precipitation Analysis for Operational Hydrological Applications in Australia: Data Sources, Methodologies, and Recommendations, WIREs Water, 12, e70037, https://doi.org/10.1002/wat2.70037, 2025.